






ARTICLE

Cell-derived and enzyme-based decellularized extracellular matrix exhibit compositional and structural differences that are relevant for its use as a biomaterial

Svenja Nellinger¹  | Ivana Mrcic² | Silke Keller^{3,4}  | Simon Heine¹  |
Alexander Southan⁵  | Monika Bach⁶ | Ann-Cathrin Volz¹ | Thomas Chassé² |
Petra J. Kluger⁷ 

¹Reutlingen Research Institute, Reutlingen University, Reutlingen, Germany

²Institute of Physical and Theoretical Chemistry, Eberhard Karls University Tübingen, Tübingen, Germany

³3R-Center for In Vitro Models and Alternatives to Animal Testing, Eberhard Karls University Tübingen, Tübingen, Germany

⁴Department for Microphysiological Systems, Institute of Biomedical Engineering, Faculty of Medicine of the Eberhard Karls University Tübingen, Tübingen, Germany

⁵Institute of Interfacial Process Engineering and Plasma Technology, University of Stuttgart, Stuttgart, Germany

⁶Biomedicine and Materials Sciences, Natural and Medical Sciences Institute at the University of Tübingen, Reutlingen, Germany

⁷School of Applied Chemistry, Reutlingen University, Reutlingen, Germany

Correspondence

Petra J. Kluger, School of Applied Chemistry, Reutlingen University, Alteburgstr. 150, 72762 Reutlingen, Germany.

Email: petra.kluger@reutlingen-university.de

Funding information

Peter and Traudl Engelhorn Foundation; Ministry of Science, Research and the Arts, Baden-Württemberg, Germany; German Science Foundation, Grant/Award Number: INST37/829-1FUGG

Abstract

Due to its availability and minimal invasive harvesting human adipose tissue-derived extracellular matrix (dECM) is often used as a biomaterial in various tissue engineering and healthcare applications. Next to dECM, cell-derived ECM (cdECM) can be generated by and isolated from in vitro cultured cells. So far both types of ECM were investigated extensively toward their application as (bio)material in tissue engineering and healthcare. However, a systematic characterization and comparison of soft tissue dECM and cdECM is still missing. In this study, we characterized dECM from human adipose tissue, as well as cdECM from human adipose-derived stem cells, toward their molecular composition, structural characteristics, and biological purity. The dECM was found to exhibit higher levels of collagens and lower levels of sulfated glycosaminoglycans compared with cdECMs. Structural characteristics revealed an immature state of the fibrous part of cdECM samples. By the identified differences, we aim to support researchers in the selection of a suitable ECM-based biomaterial for their specific application and the interpretation of obtained results.

KEYWORDS

adipose-derived stem cells, biomaterial, cell-derived matrix, decellularization, extracellular matrix

This is an open access article under the terms of the Creative Commons Attribution-NonCommercial License, which permits use, distribution and reproduction in any medium, provided the original work is properly cited and is not used for commercial purposes.

© 2022 The Authors. *Biotechnology and Bioengineering* published by Wiley Periodicals LLC

1 | INTRODUCTION

For healthcare applications (e.g., tissue-engineered implants, innovative wound dressing, coating of devices, or bioinks for bioprinting approaches) good biocompatibility of a biomaterial is a necessity. The next level in the performance of a biomaterial is its bioactivity, which enables the materials to support and enhance regeneration or cell ingrowth. One very promising material with bioactive characteristics is the harvested extracellular matrix (ECM). The ECM represents the natural environment of cells. It is a fibrous network of proteins, proteoglycans, and glycosaminoglycans (GAGs), arranged in a highly tissue-specific manner and is produced and secreted by the resident cells (Frantz et al., 2010; Mecham, 2012; Theocharis et al., 2016). This results in the establishment of specialized local microenvironments, which contribute to the differentiation and maintenance of tissue-specific cellular phenotypes and functions. Cells recognize the chemical and mechanical cues provided by ECM via membrane receptors (e.g., integrins) that trigger intracellular signaling cascades resulting in the expression of genes that regulate cellular survival, proliferation, migration, differentiation, and apoptosis (Daley & Yamada, 2013). Reciprocally, resident cells are rebuilding and remodeling the surrounding ECM by biochemical modification (e.g., cross-linking), degradation, and reassembly (P. Lu, Takai, et al., 2011). Furthermore, bioactive molecules derived from cells can be stored in and released from the ECM when necessary (Brizzi et al., 2012). These processes are tightly regulated during tissue development, homeostasis, and aging as well as in response to injury (Frantz et al., 2010; Miller et al., 2020; Rousselle et al., 2019).

Great efforts were made to develop synthetic biomaterials mimicking native ECM. However, given the complexity of ECM and the incomplete understanding of its composition and structure, fabricating materials that fully mimic the structure and composition of native ECM is very challenging. One successful method to obtain tissue-specific ECM, besides the *de novo* generation, is the decellularization of organs or tissues. A variety of different decellularization strategies have been usually described involving a combination of physical, chemical, and enzymatic treatments. Every decellularization method invariably disrupts the ECM to some degree (Thomas-Porch et al., 2018). However, human adipose tissue-derived extracellular matrix (dECM) has been extensively used as a substrate for *in vitro* cell culture systems to maintain tissue-specific cellular phenotypes and modulate cell proliferation and differentiation (Pati et al., 2014). In addition, dECM was used as a scaffold material for tissue models, which can serve as an alternative to animal testing of drugs and chemicals and as an *in vitro* model for the investigation of disease development and respective therapy approaches. In the context of the emerging field of three-dimensional (3D) bioprinting, dECM was also investigated as a component for bioinks (Kim et al., 2018; Pati et al., 2015; Tan et al., 2017; Turner et al., 2012).

For several years, an alternative method for the generation of tissue-specific ECM has moved into the focus of researchers: cell-derived ECM (cdECM). Cells produce ECM *in vitro*, which can be isolated by decellularization. Thus, cells from different tissue sources

can be used to generate (autologous) tissue-specific cdECM. Moreover, cdECM characteristics can be modulated and cdECM can be generated and maintained in a pathogen-free environment (Hussey et al., 2018; H. Lu, Hoshiba, et al., 2011). In addition, cdECM can be customized by controlling cell culture conditions like oxygen concentration, mechanical preconditioning, or specific chemical modification using metabolic glycoengineering (MGE—modification of GAGs with functional chemical groups using the natural cellular metabolism and subsequent modification with specific molecules like growth factors or enzymes) (Fitzpatrick & McDevitt, 2015; Keller, Wörgötter, et al., 2020; Ruff et al., 2017). CdECM from different tissues and developmental stages thereof can be generated by selecting specific cell types. For example, such a cdECM can be obtained by the use of, for example, mesenchymal stem cells (MSCs). These show several advantages, including high availability, functional plasticity, and low immunogenicity (C. Brown et al., 2019). Among the various sources of MSCs, adipose-derived stem cells (ASCs) represent a promising cell source for the generation of cdECM. Compared with bone marrow-derived MSCs, they can be easily obtained from adipose tissue in large quantities with little patient discomfort. Further, they exhibit a comparable differentiation potential into cells of mesodermal origin (adipogenic, osteogenic, and chondrogenic lineage) (Si et al., 2019). CdECM was investigated in a range of studies toward its influencing potential on cells and its prospective use as a biomaterial (Guneta et al., 2018). Spontaneous differentiation and subsequent loss of stem cell phenotype and genotype represent a major issue in stem cell culture. Stem cell ECM exhibits the promising potential to maintain stem cells *in vitro* by providing a stem cell-typical environment (stem cell niche) that may prevent these spontaneous differentiation events (Agmon & Christman, 2016; Novoseletskaia et al., 2019).

Both ECM sources—dECM from native adipose tissue and cdECM from cultured ASCs—are applied in healthcare biomaterial research extensively (Abaci & Guvendiren, 2020; Chiang et al., 2021; Fitzpatrick & McDevitt, 2015; Flynn, 2010; Pati et al., 2015; Rossi et al., 2018; Wolf et al., 2012). The dECM is mainly used to generate 3D tissue constructs for *in vitro* as well as *in vivo* applications (Flynn, 2010; Pati et al., 2015), whereas cdECM is particularly used for the coating of different biomaterials to enhance bioactivity or as 2D sheets (Guneta et al., 2016; Magnan et al., 2018; Rossi et al., 2018). Reviews are comparing native ECM and cdECM from different tissues (Sun et al., 2018; Sutherland et al., 2015; Xing et al., 2020). However, studies characterizing and directly comparing the composition of the ECM of different sources (native and cell-derived) and the impact on cellular behavior are missing so far. As it is well known that macromolecular, structural, and chemical features are responsible for the performance of a biomaterial, these characteristics will have to be taken into consideration when choosing the ideal biomaterial for a specific application.

In this study, dECM from native adipose tissue, as well as *in vitro*-generated cdECM (both stem cell ECM [scdECM] and adipogenic ECM [acdECM]) were characterized and compared systematically. The different ECMs were investigated in terms of their elementary

and macromolecular composition, their structural characteristic and their biological purity after processing (Figure 1). With this innovative approach, we compared the ECM of both sources directly and evaluated their potential as biomaterials for tissue engineering approaches.

2 | MATERIALS AND METHODS

All research was carried out in accordance with the rules for the investigation of human subjects as defined in the Declaration of Helsinki. Patients provided written agreement in compliance with the Landesärztekammer Baden-Württemberg (F-2012- 078, for normal skin from elective surgeries).

2.1 | Decellularization of adipose tissue

Adipose tissue samples were obtained from patients undergoing plastic surgery (Dr. Ziegler; Klinik Charlottenhaus). For their transport, tissue samples were transferred in phosphate-buffered saline with calcium and magnesium ions (PBS⁺) and were stored for a maximum of 24 h at 4°C. Decellularization was performed according to the detergent-free enzyme-based protocol published by Flynn (2010). Briefly, tissue samples were cut into pieces ranging from masses between 20 and 25 g. After three freeze-thaw cycles in hypotonic tris buffer (10 mM tris base and 5 M methylenediaminetetraacetic acid (EDTA); pH 8.0) samples were incubated in enzymatic digestion solution 1 (0.25% trypsin/0.1% EDTA) overnight, followed

by an isopropanol (99.9%) treatment for 48 h to remove lipids. Next, samples were washed three times in washing buffer (8 g/L NaCl, 200 mg/L KCl, 1 g/L Na₂HPO₄, and 200 mg/L KH₂PO₄; pH 8.0) and again treated with enzymatic digestion solution 1 for another 6 h. Subsequently, samples were washed three times and treated with enzymatic digestion solution 2 (55 mM Na₂HPO₄, 17 mM KH₂PO₄, 4.9 mM MgSO₄·7H₂O, 15,000 U DNase type II [from bovine pancreas], and 2000 U lipase type VI-S [from porcine pancreas]). Afterward, extraction of lipids was done by incubating the samples in isopropanol (99.9%) for 16 h at room temperature (RT). Last, samples were washed three times and stored in sterile PBS⁻ at 4°C. All solutions were supplemented with 1% penicillin/streptomycin (P/S).

2.2 | Generation of cell-derived extracellular matrix

ASCs were isolated from human adipose tissue samples as described before (Volz et al., 2017). ASCs were initially seeded at a density of 5×10^3 cells/cm² in a serum-free MSC growth medium (MSCGM; PELOBiotech, containing 5% human platelet lysate and 1% P/S).

For the generation of cell-derived ECM, ASCs were seeded into Petri dishes ($d = 14.5$ cm) at a density of 2.5×10^4 cells/cm² in MSCGM. At confluence, medium was changed to adipogenic differentiation medium (Dulbecco's modified eagle medium [DMEM] with 10% FCS, 1 µg/ml insulin, 1 µg/ml dexamethasone, 100 µM indomethacin, 500 µM 3-isobutyl-1-methylxanthine, and 50 µg/ml sodium ascorbate) or growth medium (DMEM with 10% FCS and 50 µg/ml sodium ascorbate). Conditioned medium exchange (half of

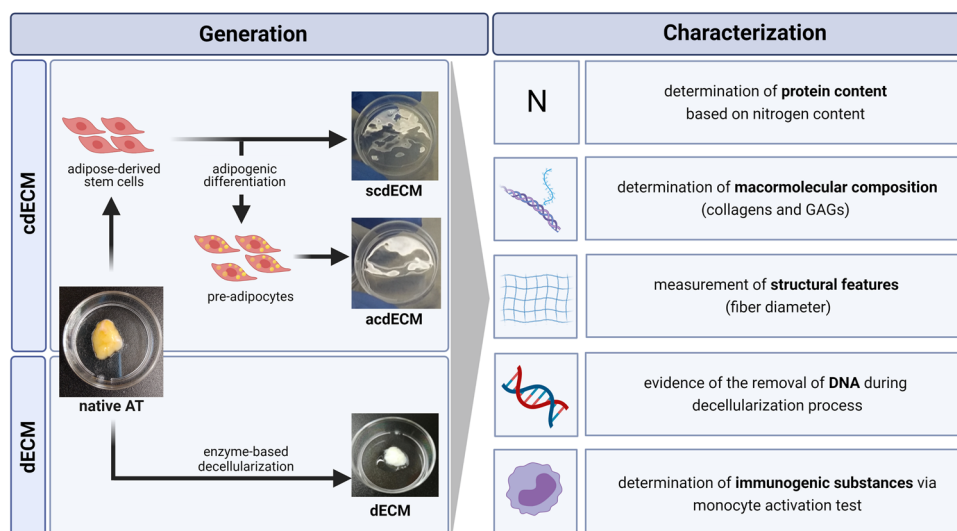


FIGURE 1 Schematic overview of the study and the performed analyses. Decellularized native extracellular matrix (dECM) was generated by enzyme-based decellularization of human native adipose tissue (AT) from human biopsies. For the generation of cell-derived ECM (cdECM), adipose-derived stem cells (ASCs) were isolated from native AT biopsies and expanded to yield an adequate cell number. Subsequently, ASCs were seeded into cell culture polystyrene dishes for the generation of cdECM and either cultured with growth medium (for generation of stem cell-derived ECM [scdECM]) or adipogenic differentiation medium (for generation of adipogenic cell-derived ECM [acdECM]). CdECM was harvested on Days 7 and 14 of cell culture. DECM and cdECM samples were analyzed for their elementary and macromolecular composition, their structural characteristics and the remaining DNA content (diameter [d] Petri dish: 35 mm). Created with BioRender.com

the medium was removed and replaced with fresh medium) was performed every second day for the approaches in adipogenic differentiation medium and complete medium exchange was performed every second day for the approaches in growth medium. On Days 7 and 14 cells were lysed using hypotonic 4 mM ammonium hydroxide solution and isolated cdECM was washed three times with ultrapure water (modified after Ruff et al. 2017). All media were supplemented with 1% P/S. ASCs were used up to passage three.

As the water content in freshly isolated cdECM is high, cdECM was concentrated using ultracentrifugation tubes (Amicon® Ultra Filter; Merck) with a molecular weight cut-off of 10 kDa (Keller, Wörgötter, et al., 2020). To achieve a homogeneous ECM solution for quantitative assays, concentrated cdECM was recovered and homogenized using lysis tubes (Lysing Matrix Z; MP Biomedicals™) and the homogenizer FastPrep-24™ 5G (MP Biomedicals™) (Keller, Wörgötter, et al., 2020). Homogenization was performed in three cycles with 60 s of lysing and a 1 min break. Keller et al. previously demonstrated that biological activity of the ECM is maintained during concentration and homogenization of cdECM (Keller, Wörgötter, et al., 2020). The dry weight of cdECM samples was determined by freeze-drying.

2.3 | Elementary analysis and X-ray photoelectron spectroscopy measurement

ECM samples were lyophilized and a minimum of 10 mg of ECM sample (dry weight) was used for the analysis following DIN EN ISO 16948 after dry combustion. Samples were burned in the oxygen stream at 900°C. During oxidative combustion, molecular nitrogen and the oxidation products CO₂, H₂O, NO, NO₂, SO₂, and SO₃ were formed from the elements C, N, and S. The resulting gas mixture was cleaned and separated into its components. The nitrogen oxides were quantitatively reduced to molecular N₂ at the copper contact in the reduction tube and then determined relatively with an accuracy of up to ±0.1% using a thermal conductivity detector (Vario El Cube; Elementar Analysensysteme GmbH). Total protein content was estimated based on the percentage nitrogen content determined by elementary analysis multiplied with the conversion range for connective tissue recommended by Keller, Liedek, et al. (2020):

$$\begin{aligned} \text{Total protein [\%]} &= \text{nitrogen content} \times 5.25 \\ &< \text{total protein} < \text{nitrogen content} \quad (1) \\ &\times 5.88. \end{aligned}$$

For X-ray photoelectron spectroscopy (XPS) analysis, concentrated cdECM and dECM samples were homogenized and 100 µl of the ECM suspension was dried at room temperature onto a silicon wafer (1 × 1 cm). The samples were measured with XPS using a multi-chamber ultrahigh vacuum system, with a base pressure of 8 × 10⁻¹⁰ mbar. The system was equipped with a Phoibos 100 analyzer and a 1d-delay line detector (SPECS). Al-Kα radiation of an Al/Mg anode (XR-50 m X-ray source, $h\nu = 1486.6$ eV) was used for the measurements. The survey spectra were collected with the following parameters: 50 eV pass energy, 0.2 s dwell time and 0.5 eV step width.

The spectral analysis was done in the software Unifit version 2018 (Unifit Scientific Software GmbH) (Hesse et al., 2004). The atomic composition was obtained from the atomic percentages, calculated with Wagner sensitivity factors (Wagner, 1983) after Shirley background subtraction. The spectra were [0.1] normalized to maximum peak height. Charge correction was done by shifting the C 1 s peak to 285.0 eV.

2.4 | Histological staining

For histological staining, dECM samples were directly fixed with 4% paraformaldehyde (10 min per 1 mm diameter of the sample; Roti Histofix; Carl Roth), cdECM samples were concentrated and afterward the yielded dense 3D cdECM construct was fixed with 4% paraformaldehyde. Fixed samples were dehydrated with ascending alcohol solutions and embedded in paraffin. Histological sections (5 µm) were produced using a microtome (Autocut 1140; Reichert-Jung). After deparaffinization and rehydration by descending alcohol solutions of histological sections, histological staining (Alcian blue PAS for the staining of proteoglycans and basal membrane and MOVAT pentachrome for the staining of elastic fibers and collagens) were performed according to the manufacturer's protocols (Morphisto GmbH). Images were taken with an Axio Observer microscope and an Axiocam 305 color using the software ZENblue (Carl Zeiss).

2.5 | Hydroxyproline and sulfated glycosaminoglycans (sGAG) assay

To determine the total collagen content of ECM samples, HP assay was performed based on Keller, Liedek, et al. (2020) and Capella-Monsonís et al. (2018). Briefly, lyophilized ECM samples were hydrolyzed overnight in concentrated hydrochloric acid at 110°C. To remove the insoluble carbohydrate fraction, samples were centrifuged at 15,000 g for 10 min. The following solutions were prepared: HP standard solutions (0, 1, 2.5, 5, 10, 20 µg/ml); diluent (isopropanol/water, 1:1); chloramine T reagent (0.2625 g chloramine T diluted in 18.75 ml), citrate buffer (17.19 g sodium acetate, 18.75 g tri-sodium citrate-dihydrate, 2.75 g citric acid diluted in 200 ml ultrapure water which afterwards was mixed with 200 ml isopropanol and brought to a final volume of 500 ml with ultrapure water); Ehrlich's reagent [2 g 4-(dimethylamino)benzaldehyde (*p*-DMAB) diluted with 3 ml 70% perchloric acid (HClO₄) and mixed with 16.7 ml isopropanol].

A total of 110 µl of samples and standard were mixed with 254 µl diluent and 176 µl chloramine T reagent, citrate buffer, and incubated at RT for 10 min. In all, 460 µl of Ehrlich's reagent was added and incubated at 70°C for 10 min. In all, 200 µl of samples and standards were transferred in a transparent 96-well plate and absorbance was measured at 555 nm (Tecan Safire 2; Tecan Trading AG). Reagent blank was subtracted from the measured values. HP content was calculated from the standard curve and the conversion range for connective tissue recommended by Keller, Liedek, et al. (2020). Collagen content was given in % of dry weight and calculated using the equation:

$$\text{Collagen content [\%]} = \text{HP content} / 0.0135$$

$$< \text{collagen content} < \text{HP content} \quad (2)$$

$$/ 0.0180.$$

To determine the content of sGAGs, lyophilized ECM samples were used for the sGAG assay according to the manufacturer's protocol (Blyscan™ Assay; Biolcolor Ltd.). Briefly, 5 mg of lyophilized samples were digested with 1 ml papain solution (0.2 M Na₂HPO₄·2-H₂O, pH 6.4, 0.4% EDTA, 0.08% cysteine HCl, 0.8% NaCH₃COO-, 0.5% papain solution; Sigma-Aldrich) at 65°C overnight. Subsequently, samples were centrifuged at 10,000 g for 10 min and the supernatant was used for the assay, which was performed according to the manufacturer's instructions. Absorbance was measured at 656 nm (Tecan Safire 2; Tecan Trading AG).

2.6 | Immunofluorescence staining

For immunofluorescence staining of ECM-specific proteins (collagen type IV and laminins), histological sections were produced according to 2.4. Deparaffinized and rehydrated sections were heat-unmasked in target retrieval buffer (pH 9.0) for 20 min in a steam cooker to unveil epitopes. Unspecific binding sites were blocked with blocking solution (3% bovine serum albumin in PBS) for 1 h at RT. Primary antibodies (rabbit-anti-Col IV [1:200]; mouse-anti-fibronectin [1:200]; rabbit-anti-Col I [1:200]; rabbit-anti-laminin [1:200]) were diluted in blocking solution and incubated for 1 h at RT. Samples were washed with washing buffer (0.1% Tween-20 in PBS) followed by incubation with the secondary antibodies (goat-anti-rabbit-AlexaFluor® 488 [1:250]; goat-anti-mouse-Cy 3 [1:250], diluted in blocking solution) for 30 min at RT. A secondary antibody control was carried along to ensure the specificity of the antibodies. Images were taken with an Axio Observer microscope and AxioCam305 color using the software ZENblue (Carl Zeiss).

2.7 | Scanning electron microscopic (SEM) analysis

Samples were fixed with 2% glutaraldehyde for 45 min at RT and dehydrated with increasing alcohol concentration followed by treatment with hexadimethylsiloxane. After incubation, samples were air-dried at RT. Samples were sputtered with platinum (Argon, 0.05 mbar, 50 s, 65 mm distance, 40 mA/470 V, 17°C; SCD 050; Balzers). SEM images were taken using a Hitachi SU8030 (Hitachi). The images were acquired using secondary electrons (SE) with an upper detector (U), 1.0 kV acceleration voltage of the electron beam, and a magnification of ×50.0 k.

2.8 | Degree of swelling

To determine the degree of swelling, lyophilized ECM samples were weighed (=dry weight). After incubation, in deionized water for 24 h, samples were weighed again (=wet weight) and the degree of swelling was calculated with the equation:

$$\text{Degree of swelling [\%]} = \frac{\text{wet weight} - \text{dry weight}}{\text{dry weight}} \times 100 \quad (3)$$

2.9 | DNA quantification

Homogenized ECM samples were treated with 1500 U/ml DNase (DNase I from bovine pancreas; Roche) at 37°C overnight. The remaining DNA in untreated and treated ECM samples was isolated by the DNA extraction kit for tissue samples (GeneOn GmbH). For qualitative assessment of the DNA content, hematoxylin and eosin staining, as well as 4,6-diamidino-2-phenylindole (DAPI) staining of sections prepared according to 2.4, was performed. Photometric quantification of the DNA content per mg dry weight in ECM samples was performed using a picogreen staining (Pico488; Lumiprobe GmbH) according to the manufacturer's instructions. As a standard for double-stranded DNA (dsDNA), lambda-DNA (Fisher Scientific GmbH) was used.

2.10 | Statistics

Elementary analysis and qualitative experiments (staining and SEM) were performed once with samples from three different biological donors ($n = 3$). All other quantitative experiments were performed three times, using samples from three different biological donors ($n = 9$). Data were analyzed by one-way analysis of variance (ANOVA) with a Bonferroni posthoc test using Origin 2018b. Statistical significances were stated as $p < 0.05$ (*), very significant as $p < 0.01$ (**), and highly significant as $p < 0.001$ (***)

3 | RESULTS AND DISCUSSION

3.1 | Quantification of total protein content

In a study comparing widely used bioanalytical methods for the characterization of ECM materials, Keller et al. demonstrated that colorimetric assays are not suitable for the determination of the total protein content of ECM materials. Instead, the estimation of total protein based on total nitrogen content provided the most reliable results (Keller, Liedek, et al., 2020). In this study, elementary and XPS analyses were performed for the estimation of the total protein content of dECM, acdECM, and scdECM as a bulk material and as a coating. By elementary analysis, the mass fraction of nitrogen (N) of the bulk material was determined (Table 1). From the relative amount of nitrogen, the amount of protein in the individual samples could be estimated using Equation (1) according to Keller, Liedek, et al. (2020). In their study, Keller et al. demonstrated that one specific conversion factor derived from the composition of only one ECM protein component is not sufficient to describe the complex composition of ECM. Thus, they recommended stating the protein content in a tissue-specific range. The used range includes the conversion factors for

TABLE 1 Protein content of dECM and cdECM samples

	Elementary analysis		XPS analysis	
	N (%)	Calc. protein content (%)	N [%]	Calc. protein content [%]
dECM	8.1 (±3.7)	42.6 (±19.2)–47.7 (±21.5)	5.0 (±0.2)	26.1 (±0.8)–29.2 (±0.9)
acdECM	7.0 (±1.4)	36.9 (±7.5)–41.3 (±8.4)	5.1 (±1.0)	27.0 (±5.4)–30.2 (±6.0)
scdECM	9.9 (±0.2)	52.3 (±0.9)–58.6 (±1.0)	4.3 (±0.7)	22.8 (±3.8)–25.5 (±4.3)

Note: Elementary analysis: ECM samples were lyophilized and elementary analysis was performed using the bulk material. XPS analysis: Concentrated and homogenized ECM samples were dried onto silicon wafers and the coating was analyzed by XPS. From the determined percentage of nitrogen, the percentage of protein content was calculated using Equation (1) ($n = 3$).

Abbreviations: acdECM, adipogenic extracellular matrix; cdECM, cell-derived extracellular matrix; dECM, human adipose tissue-derived extracellular matrix; ECM, extracellular matrix; scdECM, stem cell extracellular matrix.

collagen type I (5.25), collagen type III (5.31), collagen type IV (5.69 [$\alpha 1$]), fibronectin (5.88), and laminins (5.66). It was shown that the conversion factors for native connective tissue also lie within this range (Keller, Liedek, et al., 2020). In this study, the calculated range of protein content for dECM was found to be 42.6 (±19.2)%–47.7 (±21.5)% and lied between the ranges of acdECM with 36.9 (±7.5)%–41.3 (±8.4)% and scdECM with 52.3 (±0.9)%–58.6 (±1.0)%. As expected, the calculated protein content of scdECM is comparable to the results of Keller et al. who obtained a protein content of 53 (±4)%–59 (±4)% in ECM derived from human dermal fibroblasts. For dECM and acdECM d14 slightly lower amounts of nitrogen and consequently protein content were measured. At the same time, measured nitrogen content in dECM showed a higher variance. The higher standard deviations may indicate impurities in the dECM and acdECM samples or may highlight high donor-dependent variations in the composition of the ECMs caused by differences in the expression profile during adipogenic differentiation (Gregoire et al., 1998). However, to date, we have no conclusive explanation for this phenomenon.

XPS analysis was performed to analyze the elementary composition of ECM coatings. XPS is a surface-sensitive method with an information depth of 7–9 nm. The atomic percentages calculated from the XPS spectra are essentially the elementary composition of the ECM surface layers. In Table 1 the results of the XPS analysis are shown. Results indicate that there is no difference in the total protein content within the ECM samples. Complete results of XPS analysis including carbon percentages and results of cdECM from Day 7 are shown in Figure S1. The XPS analysis generally showed lower amounts of protein content. As shown in Figure S1 the carbon percentage is comparable in all samples. Thus the lower nitrogen/protein content measured in the XPS analysis compared with the results of the elementary analysis can be explained by atmospheric contaminations of, for example, carbon containing compounds (Graubner et al., 2004; Mrsic et al., 2021). These contaminations are caused by the adsorption of molecules from the surrounding atmosphere onto the samples during preparation. As XPS is a surface-sensitive method, these contaminations lead to a reduced detection of other elements, like nitrogen. This may result in an underestimation of their elemental contents as observed in our case. The joint consideration of the

nitrogen/protein quantification results from both methods leads to the expectation that there are no appreciable differences in protein content between the ECM samples. However, further studies should investigate this more comprehensively. Further methods like quantification of amino acids or mass spectrometry might help to get more consistent results.

3.2 | Macromolecular composition

In addition to the elementary analysis of ECM samples, their macromolecular composition was determined. To detect possible changes in composition during growth and adipogenic differentiation of cdECM, additional samples from Day 7 were examined. To get an impression of the macromolecular composition of ECM samples, histological staining was performed. For histological characterization of important extracellular structures, Alcian blue PAS and MOVAT pentachrome staining were done (Figure 2A). By Alcian blue PAS, proteoglycans are stained in blue and the basal membrane is stained in purple. The basal membrane is an extracellular matrix structure that separates epithelial or endothelial tissues from the underlying stroma (Randles et al., 2017). It can further be found around adipocytes in mature AT (Pierleoni et al., 1998). dECM exhibited large parts of the preserved basal membrane (purple). No basal membrane, but high amounts of proteoglycans (blue) was found in cdECM samples. Based on the histological staining it can be presumed that there is no difference in proteoglycan composition and distribution between the different cdECM samples. By MOVAT pentachrome staining, ground substance (non-fibrous components like proteoglycans and glycosaminoglycans [green]), collagens (yellow), and elastic fibers (black) were stained. A high amount of ground substance and collagens was found in dECM. Furthermore, elastic fibers were observed in dECM samples. In all cdECM samples, high amounts of ground substance but no elastic fibers were found. The absence of elastic fibers in cdECMs leads to the assumption that these cdECMs exhibit an immature state of development. This can be explained by several studies which have shown before that in the absence of mechanical stimuli elastin synthesis and formation of elastic fibers are lower in vitro (Eoh et al., 2017; Hinderer et al., 2015). Overview

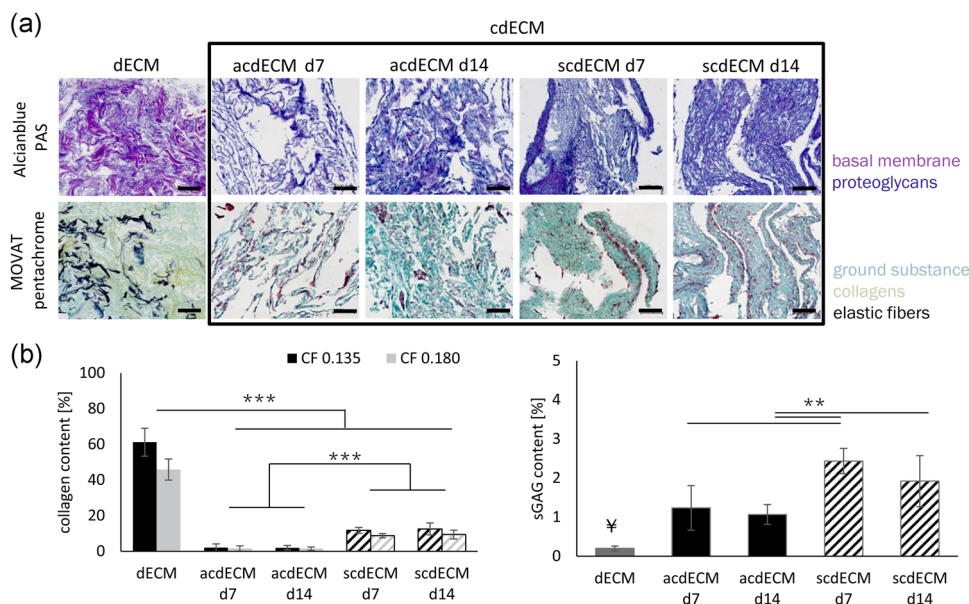


FIGURE 2 Macromolecular composition of ECM samples. (A) Histological staining: Alcian blue PAS and MOVAT Pentachrome staining were performed on histological sections of dECM, acdECM, and scdECM samples. Alcian blue PAS staining: proteoglycans (blue) and basal membrane (purple). MOVAT Pentachrome staining: ground substance (green), collagen (yellow), and elastic fibers (black) (scale bars: 100 μ m; $n = 3$) B: Quantification of collagens and sGAGs: Collagen content in ECM samples was determined via HP assay and was normalized to the dry weight (DW) of the sample (CF, conversion factor). The amount of sGAGs was determined by a colorimetric sGAG assay and normalized to the DW. $**p \leq 0.01$; $***p \leq 0.001$; $^{\#}p \leq 0.001$ to all other samples; $n = 9$. acdECM, adipogenic extracellular matrix; dECM, human adipose tissue-derived extracellular matrix; ECM, extracellular matrix; scdECM, stem cell extracellular matrix; sGAG, sulfated glycosaminoglycans

staining with hematoxylin and eosin (HE) and a picrosirius staining (for the visualization of the homogenous distribution of collagens in all samples) is shown in Figure S2.

In the next step, the two main components of ECM—collagens and sGAGs—were quantified (Figure 2B). Results were normalized to the dry weight (DW) of the samples and given in percent. For quantification of collagen content, a hydroxyproline (HP) assay was performed and collagen content was calculated based on this assay. The amino acid HP is mainly contained in collagens and only to a limited amount in elastin (Capella-Monsonís et al., 2018). Thus, the HP content can be used for the quantification of collagens. For the calculation, the conversion range from 0.135 to 0.180 was used, based on the findings of Keller et al. The used conversion range includes the conversion factors for collagen type I (0.135) and collagen type III (0.180). The conversion factors for native connective tissue lie also within this range (Keller, Liedek, et al., 2020). Results indicated a significantly higher amount of collagens in dECM [45.9 (± 5.9)%–61.2 (± 7.9)%] compared with all cdECM samples. Within the cdECM approaches, significantly higher collagen content was found in scdECM samples [scdECM d7: 8.8 (± 1.2)%–11.8 (± 1.6)%, scdECM d14: 9.4 (± 2.5)%–12.6 (± 3.3)%] compared with the acdECM samples [acdECM d7: 1.6 (± 1.5)%–2.1 (± 2.0)%, acdECM d14: 1.5 (± 0.9)%–2.0 (± 1.2)%]. These results are in line with the MOVAT pentachrome staining (collagens stained in yellow) with the most intense staining in dECM. The amount of collagens in scdECM samples found in this study are in the same order of magnitude as the values shown by Keller et al. with 12%–16% in cdECM from juvenile human skin fibroblasts (Keller, Liedek, et al., 2020). Interestingly, the HP assay revealed the highest collagen

content to be present in dECM and the lowest collagen content in acdECMs. One reason why we observed higher collagen content in dECM might be the presence of elastic fibers, which were only found in dECM (see histological staining) and which contain little amounts of HP. However, that does not explain the enormous differences between dECM and cdECM samples. A further explanation might be the maturing/culture period. The dECM has grown over several years, whereas the cdECM was generated in only 7–14 days in vitro. During collagen synthesis, tropocollagen is secreted by the cells and assembled extracellularly to form mature collagen fibers (Myllyharju & Kivirikko, 2004). In native tissue, collagen fibers are completely polymerized and may be preserved during decellularization. In cell culture, the tropocollagen is partly released into the cell culture medium or loosely attached to the cell surrounding and may get lost during medium exchange and decellularization (Shendi et al., 2019). The differences in collagen content between acdECM and scdECM samples could be explained by alterations in protein expression during adipogenic differentiation. The relative concentrations of collagen type I and collagen type III decline by 80%–90% during adipogenic differentiation and the secretion of collagen type IV and the glycoprotein nidogen increases (Aratani & Kitagawa, 1988; Gregoire et al., 1998). As the interactions of cells and ECM proteins play a pivotal role in cellular development and behavior, these differences should be considered when choosing a material for a specific application.

Quantification of sGAGs revealed a significantly lower amount in dECM [0.20 (± 0.06)%] compared with all cdECM approaches. Within the cdECM approaches, scdECM d7 [2.43 (± 0.32)%] exhibited a significantly higher amount of sGAGs compared with both acdECM

approaches [acdECM d7: 1.24 (± 0.57)%, acdECM d14: 1.07 (± 0.25)%]. Further, the sGAG content of scdECM d14 [1.92 (± 0.65)%] was significantly higher compared with acdECM d14.

As it is well known that sGAGs have a positive impact on cellular behavior regarding regenerative capacity and angiogenesis/neovascularization, which remains a major obstacle in tissue engineering (Köwitsch et al., 2018; Salbach et al., 2012), ECMs containing higher amounts of sGAGs, which are on top preserved during decellularization would be favorable. The noticeable low amount of sGAG in dECM could be explained by the harsh decellularization method used for native tissue. GAGs are known to be very sensitive to a variety of agents used in decellularization protocols (B. N. Brown et al., 2011; Crapo et al., 2011). The reported amount of preserved sGAGs in dECM from human adipose tissue ranges from 0.05% up to 0.4% (Song et al., 2018; L. Wang et al., 2013; Young et al., 2011). Reported sGAG content in different native human tissues range from 0.3% to 0.7% (Eckert et al., 2013; Johnson et al., 2014; Wei et al., 2005). This indicates a loss of sGAGs during decellularization of up to 70% in our study. However, the high amount of lipids within AT seems to interfere with the reliable determination of sGAGs in native AT. The available data about the sGAG content in native AT and on the reduction of sGAGs during decellularization of native AT is rare and varies extremely. Song et al. (2018) found no significant reduction of sGAGs after decellularization, whereas Pati et al. (2014) described a reduction of about 60%. In general, the usually performed normalization of the values to the dry weight leads to questionable comparability of native and decellularized tissue, since the removal of cellular components leads to distorted values. In this study, we found that cdECM represents a promising alternative to dECM, as the amount of sGAGs is up to 12-fold higher in scdECM from Day 7 compared with dECM. Previously, Schenke-Layland et al. (2009) found 3.1% of sGAGs in non-decellularized fibroblast-derived ECM sheets, which indicates adequate preservation of sGAGs in cdECM during the decellularization process in our study. Keller, Liedek, et al. (2020) investigated the sGAG content in fibroblast-derived ECM. Compared with their results (2.4%) the amount of sGAG determined

in this study was found to be in the same order of magnitude. As GAGs are known to exhibit a positive influence on cellular behavior in regenerative processes (e.g., proliferation, vascularization), cdECM containing and preserving higher amounts of GAGs represent a promising material in regenerative applications.

3.3 | Expression of proteins associated with basal membrane

The basal membrane plays a fundamental role in cellular anchorage, as a physical barrier, and in signaling (Leclech et al., 2021). Thus, the preservation of basal membrane structures during decellularization would be beneficial for healthcare approaches. Histological staining suggested the presence of superordinate structures, like the basal membrane, in dECM, but not in cdECM samples (Figure 2). Two of the main components of the basal membrane are collagen type IV and laminins (Kalluri, 2003; Yurchenco & Schittny, 1990). In the next step, the presence of these basal membrane-associated ECM proteins collagen type IV and laminins, was proven by an immunofluorescence staining (Figure 3). After decellularization, a heterogeneous distribution of dense and loosely packed structures was observed in dECM. For all cdECM approaches—regardless of the time point of isolation—densely packed structures with ubiquitous staining of ECM-specific proteins were found. Qualitative analysis of the immunofluorescence images did not indicate differences between the investigated ECM samples. This indicates that basal membrane proteins are also present in cdECM but do not exhibit the specific structure of the basal membrane, which might prevent the binding of the dye in histological staining. Immunofluorescence staining of ECM-specific proteins collagen type I and fibronectin are shown in Figure S3.

Previous studies demonstrated that laminin, which is mainly found in the basal membrane, contributes to the formation and maintenance of vascular structures (MALINDA et al., 1999; Ponce et al., 1999). After homogenization, which is necessary for further

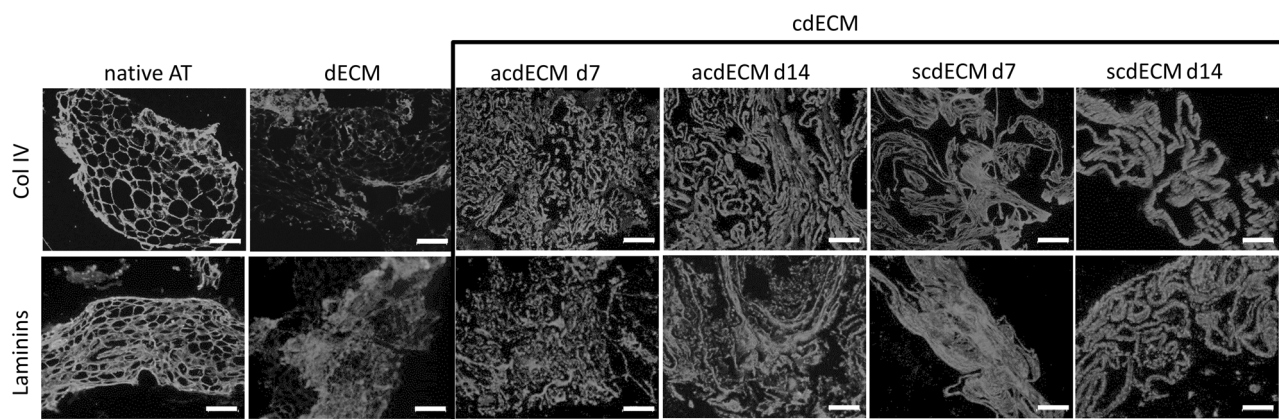


FIGURE 3 Immunofluorescence staining of basal membrane proteins collagen type IV and laminins. The presence of proteins collagen type IV and laminins were proven by immunofluorescence staining (Scale bar: 200 μ m; $n = 3$)

processing as biomaterial, the structure of the basal membrane is very likely disrupted in all ECM samples. Thus, the presence of basal membrane proteins (e.g., collagen type IV and laminins) may play a stronger role than the specific structure of the basal membrane. If a well-developed basal membrane as a biomaterial is desired epithelial or endothelial cells, that mainly produce basal membrane *in vivo* and *in vitro*, in monoculture or coculture with other cell types can be used. This is especially useful for the coating of synthetic materials when the original structure can be restored and is not disrupted by further processing of a harvested cdECM (Carvalho et al., 2019; Junka et al., 2020). Dao Thi et al. (2020) recently described a method to polarize stem cells using a growth factor gradient in trans wells yielding hepatocyte-like cells with an apical and a basolateral side. Despite *in vivo* adipocytes does not exhibit this polarization this method might be promising to enhance basal membrane secretion of cdECM.

3.4 | Structural characterization

Topographical characteristics are known to strongly influence cellular behavior such as proliferation and differentiation (Ko et al., 2016; Shi et al., 2014; Z. Wang et al., 2016). For example, Abagnale et al. showed that ASCs, without specific differentiation media, underwent osteogenesis on 2 μm thick microfibers but adipogenesis on microfibers with a diameter of 15 μm . However, no upregulation of specific differentiation markers was observed on fiber diameters thinner than 400 nm (Abagnale et al., 2015). Fiber diameter as the primary topographical feature of fibrous materials such as ECM was evaluated by SEM. In Figure 4, SEM images of the dECM and cdECM are shown. A significantly higher fiber diameter in dECM [63.9 (\pm 12.8) nm] compared with cdECM samples [acdECM d7: 35.9 (\pm 9.2) nm; acdECM d14: 37.7 (\pm 11.2) nm; scdECM d7: 36.7 (\pm 7.7) nm; scdECM d14: 37.3 (\pm 11.2) nm] was observed. The immature state of collagen fibers in cdECM previously indicated by the histological staining (Figure 2) could also be observed in the SEM analysis. The mature collagen

fibers of dECM exhibited the characteristic cross stripes with an average distance of 65 nm (black arrows), derived from the assembly of the tropocollagen molecules, whereas no stripes were found in cdECM samples.

The influence of these features on cell fate has to be considered when using the materials for specific applications and if necessary soluble factors are needed to prevent unwanted differentiation events. As longer culture periods are not practicable for the generation of a biomaterial, different culture methods, such as macromolecular crowding, hypoxia, reduced frequency of medium replacement, and reduction of serum concentration can be tested to increase the maturity and diameter of the collagen fibers of cdECM, if needed (Assunção et al., 2020). The period for the generation of a biomaterial that can be assumed to be suitable strongly depends on the intended use. For the generation of cdECM, which is used for *in vitro* applications (e.g., the built-up of tissue models) and *in vivo* application where it can be generated in advance (allogenic products) culture periods of a few weeks can be seen as feasible. In contrast for the treatment of patients with autologous material, only generation periods of a few days can be seen as feasible.

3.5 | Degree of swelling

The degree of swelling describes the ability of a material to bind water, which has a high impact on the materials' physical properties. The ability of a material to bind water depends on structural characteristics (e.g., pore size) and chemical properties (e.g., charge). Thus, differences in the degree of swelling indicate differences in structural and chemical material characteristics. Figure 5 shows the degree of swelling of dECM and cdECM samples. It was found that acdECM from both time points [acdECM d7: 2357.6 (\pm 201.1)% (this value was already published by us in Nellinger et al. 2020) and acdECM d14: 2329.4 (\pm 118.7)%] exhibited a higher degree of swelling compared with dECM [1288.1 (\pm 383.3)%]. Further, acdECM exhibited a higher degree of swelling compared with scdECM d7 [scdECM d7: 1624.3

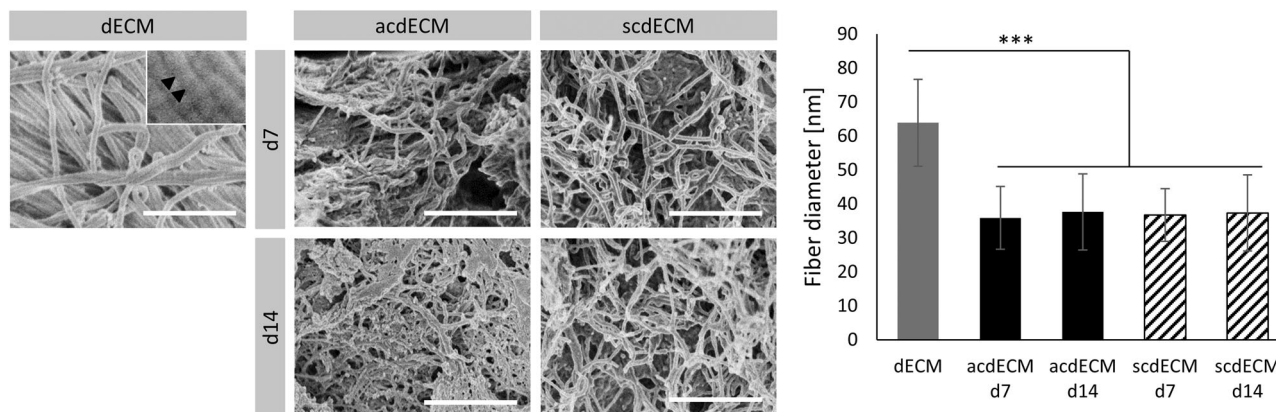


FIGURE 4 Analysis of fiber diameter of the different ECM samples: Fiber diameter was determined with ImageJ using SEM images of ECM samples ($n = 9$). Black arrows: horizontal stripes with a distance of 65 nm (scale bar: 1 μm ; *** $p \leq 0.001$). ECM, extracellular matrix; SEM, scanning electron microscopy

(±96.4)% (this value is already published by us in Nellinger et al. 2020)] independent of the day. The degree of swelling of scdECMd14 [1764.5 (±421.0)%] was significantly lower compared with acdECM d7, within the different evaluation days of cdECM.

One possible explanation for the differences in the degree of swelling between the ECM samples is different degrees of cross-linking. A higher degree of cross-linking leads to a lower swelling degree. With the results of this study, it can be assumed that with the higher collagen content the degree of cross-linking is higher in scdECM samples compared with acdECM, leading to a lower degree of swelling in scdECM samples. Interestingly, the swelling degree of dECM was found to be comparable to scdECM. This might be explained by the mature state of dECM (as demonstrated by SEM) and therefore a higher degree of cross-linking compared with acdECM.

It is well known that physical characteristics influence cellular behavior strongly (Engler et al., 2006; Kshitz et al., 2012). For example, Guneta et al. (2016) demonstrated increased proliferation and adipogenic differentiation of ASCs on alginate scaffolds with decreasing stiffness. Furthermore, Subbiah et al. (2016) showed that an increase of cross-linking of cdECM is accompanied by a rise of stiffness and a shift from adipogenic differentiation to osteogenic differentiation. Considering these results, it can be assumed that acdECM, produced in this study, may also favor adipogenic differentiation, whereas scdECM and dECM may favor chondrogenic and osteogenic differentiation. Thus, next to the structural characteristics, the degree of swelling of the ECMs must be considered when using ECM as a biomaterial to prevent unwanted differentiation events.

3.6 | DNA content

Removal of DNA is a critical indicator for successful decellularization. It is known that remaining DNA can contribute to cytocompatibility problems and immunogenic reactions upon reintroduction of cells (B. N. Brown et al., 2009). A limit of residual DNA for its use as biomaterial is not officially defined, however, the postulated limit of

50 ng/mg by Capro et al. is generally accepted (Crapo et al., 2011). The absence of remaining DNA in decellularized cdECM and dECM samples was proven by a HE and DAPI staining for qualitative evidence and by a Pico488 assay for quantitative evidence. In Figure 6, histological stainings of dECM and scdECMd7 are exemplarily shown. The HE staining revealed a strong decrease of DNA (blue/purple) for both approaches after treatment with DNase (w/DNase) compared with the samples without DNase treatment (w/o DNase). In addition, DAPI staining indicated a strong reduction of the nucleic acid content in samples treated with DNase compared with untreated samples. Untreated and DNase treated dECM and cdECM samples exhibited a DNA content below the postulated limit of 50 ng/mg DW in the treated samples. For dECM samples a significantly lower amount of DNA was observed [7.9 (±4.5) ng/mg] compared with all cdECM approaches [acdECM d7: 37.0 (±17.8) ng/mg; acdECM d14: 46.0 (±2.9) ng/mg; scdECM d7: 28.4 (±22.8) ng/mg; scdECM d14: 43.2 (±4.5) ng/mg] after the treatment with DNase.

The variation of DNA content in untreated ECM of the different origins was most likely caused by the difference in the present cell number in the samples. Due to the large portion of big mature adipocytes in native AT, it exhibited the lowest total cell number per volume, whereas the cdECM approaches proportionally exhibited a higher number of cells resulting in a higher amount of remaining DNA in the decellularized samples.

4 | GENERAL ASPECTS

Due to their different appearance, the decellularization protocols of the two ECMs differ in the used solutions and time by default in current studies (Flynn, 2010; Guneta et al., 2018; Magnan et al., 2018, 2021; Song et al., 2018). In this study, dECM was decellularized using relatively harsh chemicals and enzymes (no detergents which are classified as critical were used) whereas cdECM was treated with a relatively gentle hypotonic solution and nucleases. It is to be assumed that this will have a great impact on some of the obtained results in this study (preservation of GAGs and the degree of swelling). However, in our opinion, this would rather be another reason for the use of cdECM whenever possible. This would, further, have the advantage that no chemicals remain in the material that could have a potentially negative effect on cells *in vivo* or *in vitro*.

Next to the demonstrated characteristics and differences also general aspects, such as costs of production, mechanical properties, and tunability have to be considered when choosing between dECM and cdECM as a biomaterial. Native adipose tissue can be harvested with low invasiveness in relatively high amounts and frequently is a waste product from plastic surgery. Depending on the used protocol the decellularization process includes the treatment with costly enzymes. However, relatively high amounts of dECM can be achieved with little effort. In contrast, the culture of ECM producing cells over several weeks with the needed consumables and media supplements is much more expensive. Especially since the yielded amount of cdECM which can be produced in one cell culture flask or plate is

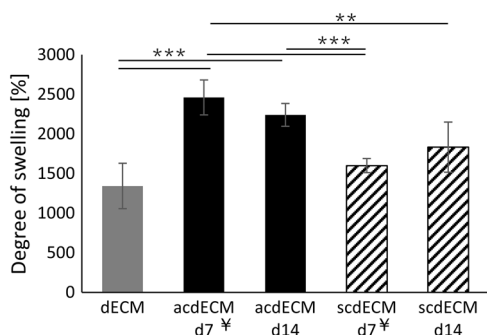


FIGURE 5 Degree of swelling. The degree of swelling was calculated from the dry and wet weight of ECM samples according to Equation (3) and displayed in percentual amount (¥ = data from Nellinger et al., 2020; ** $p \leq 0.01$; *** $p \leq 0.001$; $n = 9$). ECM, extracellular matrix

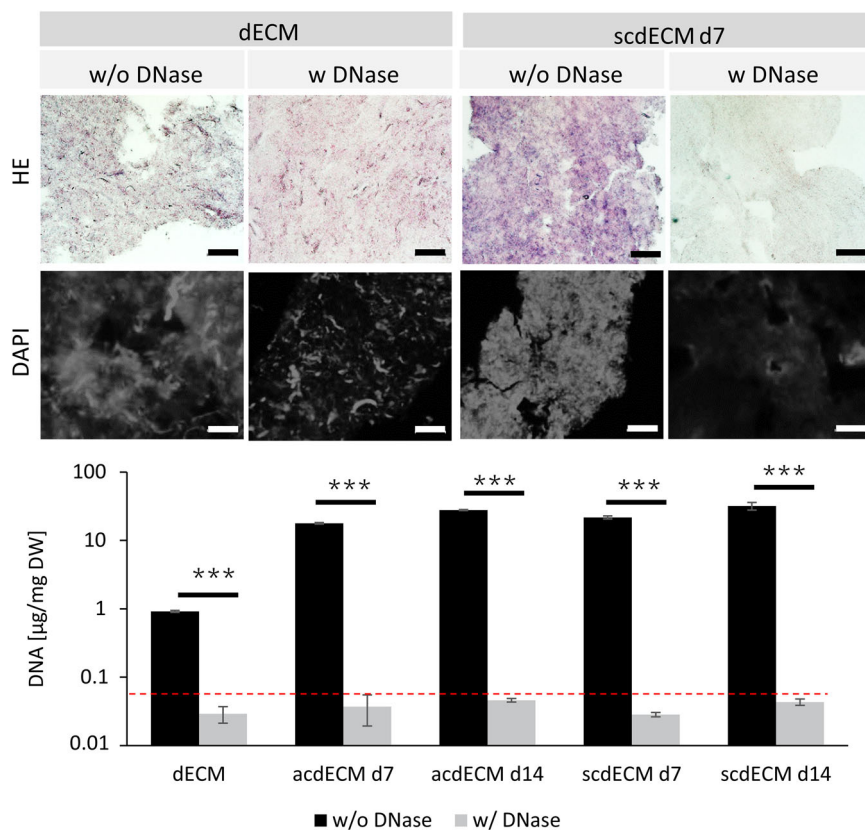


FIGURE 6 DNA content after treatment with DNase. To remove the remaining DNA, ECM samples were treated with 1500 U/ml of DNase. To determine DNA content in ECM samples, HE and DAPI staining were performed on histological sections of ECM samples with and without DNase treatment ($n = 3$). Quantification of total DNA content in DNase-treated ECM samples was performed using Pico488. $***p \leq 0.001$; red dotted line: 50 ng/mg DW; $n = 9$. DAPI, 4,6-diamidino-2-phenylindole; DW, dry weight; ECM, extracellular matrix; HE, hematoxylin and eosin

extremely low. Thus, the upscaling of cdECM production is a key step toward its widespread use in tissue engineering and healthcare. Next to the usual supplemented sodium L-ascorbate that increases collagen secretion, further methods are known to enhance cdECM yield. These include pharmaceutical substances that affect cellular pathways (e.g., TGF- β pathway that was shown to cause increased ECM secretion [Biancheri et al., 2014]) and genetic alterations that lead to overexpression of ECM proteins (Chan et al., 2021). However, as these techniques are extremely invasive the resulting cdECMs need to be carefully studied before being used for biomedical applications. A less invasive method that is currently used is macromolecular crowding which enhances the polymerization of collagen fibers extracellularly.

For further processing it is necessary for both ECMs to homogenize the material except the original shape is sought to be reseeded with cells. For tissue engineering and healthcare applications in most cases, the original shape does not need to be restored. When the ECM is blended with another (hydrogel)material or used as a coating it has to be homogenized to achieve a homogeneous distribution of the ECM with the hydrogel or on the surface. Thus, the mechanical properties of the ECM material itself can be more or less neglected. Regarding the tunability of the ECM, cdECM brings a great advantage as it can be equipped with specific addressable functional groups using metabolic glycoengineering (MGE) (Gutmann et al., 2018; Ruff et al., 2017). During MGE the cells metabolize a modified sugar derivative and incorporate it into the glycocalyx and the ECM. The functional group can then be used to covalently and site-directed link

bioactive molecules, like growth factors, or can be used to crosslink the ECM with another material or with itself in a controllable manner. In contrast, the modification of native unmodified dECM occurs randomly and is not site-directed which may impact the effect of the bioactive molecules by covering the bioactive epitope(s). Further, the modification and crosslinking of dECM is performed with chemicals that may alter the structure of the ECM and therefore its impact on the cells when used for tissue engineering and healthcare applications (Braun et al., 2018; Subbiah et al., 2016).

One aspect which needs to be investigated in cdECM is the binding of serum proteins to cdECM structures. CdECM is produced using fetal calf serum (FCS) containing media. As it is well known that there are high batch-to-batch variations in FCS and proteins can be bound to ECM and thus remain in the material. This might be a concern regarding the reproducibility of cell experiments (Boyd & Thomas, 2017). However, also in dECM donor variations might have an impact on the outcome of in vitro and in vivo experiments. Thus, the standardization of cdECM production using defined media would turn this disadvantage of cdECM into an advantage against the dECM where the donor variation cannot be eliminated.

In future studies, dECM and cdECM from further tissues should be characterized and investigated and a more detailed investigation of ECM proteins should be performed. Due to the complexity of the ECM colorimetric assays might be error-prone (comparable to total protein quantification). A more reliable method might be mass spectrometry. This method complements the results of the present study as it enables the identification and quantification of individual proteins and allows their

classification (Johnson et al., 2016). This in turn would give more insight into the functionalities of the different ECMs. Based on further studies characterizing and comparing dECM and cdECM from different tissues, the range of methods needed to be performed to work with a well-defined ECM material can be reduced. From our point of view histological staining (Movat Pentachrome and Alcian blue PAS), quantification of sGAG, and remaining DNA represent a feasible amount of experiments that monitor the efficiency and reproducibility decellularization process and can be performed in most laboratories.

5 | CONCLUSION

In the present study, we compared dECM and cdECM from stem cells and adipogenic differentiated ASCs toward their macromolecular composition and their structural features. We found that cdECM exhibited more sGAGs which are beneficial for regenerative processes. The thinner collagen fibers and of cdECM indicate its immature state and the accompanying differences in topography might have an impact on cell fate. With the differences identified, we aim to support researchers in the decision, which ECM is suitable as a biomaterial for their specific application. The differences between the ECMs investigated have the potential to highly influence experimental outcomes and therefore should be considered when choosing a biomaterial for tissue engineering or healthcare application. Next to the found characteristics and differences, to date, general aspects, such as costs of production and possibilities in the tunability have to be considered. To find the ideal material for a specific application the aim of the planned study has to be opposed to the advantages and disadvantages of both ECM materials.

ACKNOWLEDGMENTS

We acknowledge the financial support of the Ministry of Science, Research and the Arts (Baden-Württemberg, Germany), for the University of Tuebingen and the Reutlingen University under the program "Intelligent Process and Material Development in Biomateriomics." The authors kindly thank Prof. Dr. Katja Schenke-Layland (University of Tuebingen) and Prof. Dr. Ralf Kemkemer (Reutlingen University) for the helpful discussion of the results and Isabelle Schmidt (Reutlingen University) for the support in the experimental procedure and the Analytical Chemistry Unit (University of Hohenheim) for the performance of the elementary analysis. The authors thank Elke Nadler for SEM measurements. The SEM/S (T)EM was cofounded by the German Science Foundation (DFG) under contract no. INST37/829-1FUGG. Silke Keller kindly acknowledges the Peter and Traudl Engelhorn Foundation for its financial support through her PhD scholarship. Open Access funding enabled and organized by Projekt DEAL.

CONFLICT OF INTERESTS

The authors declare that there are no conflict of interests.

DATA AVAILABILITY STATEMENT

The data that support the findings of this study are available from the corresponding author upon reasonable request.

ORCID

Svenja Nellinger  <http://orcid.org/0000-0001-7281-2196>

Silke Keller  <http://orcid.org/0000-0003-3331-6856>

Simon Heine  <http://orcid.org/0000-0002-8006-3348>

Alexander Southan  <http://orcid.org/0000-0001-7530-1690>

Petra J. Kluger  <http://orcid.org/0000-0001-6784-7378>

REFERENCES

- Abaci, A., & Guvendiren, M. (2020). Designing decellularized extracellular matrix-based bioinks for 3D bioprinting. *Advanced Healthcare Materials*, 9(24), 2000734. <https://doi.org/10.1002/ADHM.202000734>
- Abagnale, G., Steger, M., Nguyen, V. H., Hersch, N., Sechi, A., Joussem, S., Denecke, B., Merkel, R., Hoffmann, B., Dreser, A., Schnakenberg, U., Gillner, A., & Wagner, W. (2015). Surface topography enhances differentiation of mesenchymal stem cells towards osteogenic and adipogenic lineages. *Biomaterials*, 61, 316–326. <https://doi.org/10.1016/j.biomaterials.2015.05.030>
- Agmon, G., & Christman, K. L. (2016). Controlling stem cell behavior with decellularized extracellular matrix scaffolds. *Current Opinion in Solid State and Materials Science*, 20(4), 193–201. <https://doi.org/10.1016/j.cossms.2016.02.001>
- Aratani, Y., & Kitagawa, Y. (1988). Enhanced synthesis and secretion of type IV collagen and entactin during adipose conversion of 3T3-L1 cells and production of unorthodox laminin complex. *Journal of Biological Chemistry*, 263(31), 16163–16169. [https://doi.org/10.1016/s0021-9258\(18\)37573-2](https://doi.org/10.1016/s0021-9258(18)37573-2)
- Assunção, M., Dehghan-Baniani, D., Yiu, C. H. K., Später, T., Beyer, S., & Blocki, A. (2020). Cell-derived extracellular matrix for tissue engineering and regenerative medicine. *Frontiers in Bioengineering and Biotechnology*, 8, 602009. <https://doi.org/10.3389/fbioe.2020.602009>
- Biancheri, P., Giuffrida, P., Docena, G. H., MacDonald, T. T., Corazza, G. R., & Di Sabatino, A. (2014). The role of transforming growth factor (TGF)- β in modulating the immune response and fibrogenesis in the gut. *Cytokine & Growth Factor Reviews*, 25(1), 45–55. <https://doi.org/10.1016/J.CYTOGFR.2013.11.001>
- Boyd, D. F., & Thomas, P. G. (2017). Towards integrating extracellular matrix and immunological pathways. *Cytokine*, 98, 79–86. <https://doi.org/10.1016/J.CYTO.2017.03.004>
- Braun, B., Gutmann, M., Lühmann, T., & Meinel, L. (2018). Bioorthogonal strategies for site-directed decoration of biomaterials with therapeutic proteins. *Journal of Controlled Release*, 273, 68–85. <https://doi.org/10.1016/J.JCONREL.2018.01.018>
- Brizzi, M. F., Tarone, G., & Defilippi, P. (2012). Extracellular matrix, integrins, and growth factors as tailors of the stem cell niche. *Current Opinion in Cell Biology*, 24(5), 645–651. <https://doi.org/10.1016/j.ceb.2012.07.001>
- Brown, B. N., Freund, J. M., Han, L., Rubin, J. P., Reing, J. E., Jeffries, E. M., Wolf, M. T., Tottey, S., Barnes, C. A., Ratner, B. D., & Badylak, S. F. (2011). Comparison of three methods for the derivation of a biologic scaffold composed of adipose tissue extracellular matrix. *Tissue Engineering—Part C: Methods*, 17(4), 411–421. <https://doi.org/10.1089/ten.tec.2010.0342>
- Brown, B. N., Valentin, J. E., Stewart-Akers, A. M., McCabe, G. P., & Badylak, S. F. (2009). Macrophage phenotype and remodeling outcomes in response to biologic scaffolds with and without a cellular component. *Biomaterials*, 30(8), 1482–1491. <https://doi.org/10.1016/j.biomaterials.2008.11.040>
- Brown, C., McKee, C., Bakshi, S., Walker, K., Hakman, E., Halassy, S., Svinarich, D., Dodds, R., Govind, C. K., & Chaudhry, G. R. (2019). Mesenchymal stem cells: Cell therapy and regeneration potential. *Journal of Tissue Engineering and Regenerative Medicine*, 13(9), 1738–1755. <https://doi.org/10.1002/term.2914>

- Capella-Monsonís, H., Coentro, J. Q., Graceffa, V., Wu, Z., & Zeugolis, D. I. (2018). An experimental toolbox for characterization of mammalian collagen type I in biological specimens. *Nature Protocols*, 13(3), 507–529.
- Carvalho, M. S., Silva, J. C., Udangawa, R. N., Cabral, J. M. S., Ferreira, F. C., da Silva, C. L., Linhardt, R. J., & Vashishth, D. (2019). Co-culture cell-derived extracellular matrix loaded electrospun microfibrillar scaffolds for bone tissue engineering. *Materials Science and Engineering: C*, 99, 479–490. <https://doi.org/10.1016/J.MSEC.2019.01.127>
- Chan, W. W., Yu, F., Le, Q. B., Chen, S., Yee, M., & Choudhury, D. (2021). Towards biomanufacturing of cell-derived matrices. *International Journal of Molecular Sciences* 2021, 22(21), 11929. <https://doi.org/10.3390/IJMS222111929>
- Chiang, C.-E., Fang, Y.-Q., Ho, C.-T., Assunção, M., Lin, S.-J., Wang, Y.-C., Blocki, A., & Huang, C.-C. (2021). Bioactive decellularized extracellular matrix derived from 3D stem cell spheroids under macromolecular crowding serves as a scaffold for tissue engineering. *Advanced Healthcare Materials*, 10(11), 2100024. <https://doi.org/10.1002/ADHM.202100024>
- Crapo, P. M., Gilbert, T. W., & Badylak, S. F. (2011). An overview of tissue and whole organ decellularization processes. *Biomaterials*, 32(12), 3233–3243. <https://doi.org/10.1016/j.biomaterials.2011.01.057>
- Daley, W. P., & Yamada, K. M. (2013). ECM-modulated cellular dynamics as a driving force for tissue morphogenesis. *Current Opinion in Genetics and Development*, 23(4), 408–414. <https://doi.org/10.1016/j.gde.2013.05.005>
- Dao Thi, V. L., Wu, X., Belote, R. L., Andreo, U., Takacs, C. N., Fernandez, J. P., Vale-Silva, L. A., Prallet, S., Decker, C. C., Fu, R. M., Qu, B., Uryu, K., Molina, H., Saeed, M., Steinmann, E., Urban, S., Singaraja, R. R., Schneider, W. M., Simon, S. M., & Rice, C. M. (2020). Stem cell-derived polarized hepatocytes. *Nature Communications*, 11(1), 1–13. <https://doi.org/10.1038/s41467-020-15337-2>
- Eckert, C. E., Fan, R., Mikulis, B., Barron, M., Carruthers, C. A., Friebe, V. M., Vyavahare, N. R., & Sacks, M. S. (2013). On the biomechanical role of glycosaminoglycans in the aortic heart valve leaflet. *Acta Biomaterialia*, 9(1), 4653–4660. <https://doi.org/10.1016/j.actbio.2012.09.031>
- Engler, A. J., Sen, S., Sweeney, H. L., & Discher, D. E. (2006). Matrix elasticity directs stem cell lineage specification. *Cell*, 126(4), 677–689. <https://doi.org/10.1016/j.cell.2006.06.044>
- Eoh, J. H., Shen, N., Burke, J. A., Hinderer, S., Xia, Z., Schenke-Layland, K., & Gerecht, S. (2017). Enhanced elastin synthesis and maturation in human vascular smooth muscle tissue derived from induced-pluripotent stem cells. *Acta Biomaterialia*, 52, 49–59. <https://doi.org/10.1016/j.actbio.2017.01.083>
- Fitzpatrick, L. E., & McDevitt, T. C. (2015). Cell-derived matrices for tissue engineering and regenerative medicine applications. *Biomaterials Science*, 3(1), 12–24. <https://doi.org/10.1039/c4bm00246f>
- Flynn, L. E. (2010). The use of decellularized adipose tissue to provide an inductive microenvironment for the adipogenic differentiation of human adipose-derived stem cells. *Biomaterials*, 31(17), 4715–4724. <https://doi.org/10.1016/j.biomaterials.2010.02.046>
- Frantz, C., Stewart, K. M., & Weaver, V. M. (2010). The extracellular matrix at a glance. *Journal of Cell Science*, 123(24), 4195 LP–4200. <https://doi.org/10.1242/jcs.023820>
- Graubner, V. M., Jordan, R., Nuyken, O., Schnyder, B., Lippert, T., Kötz, R., & Wokaun, A. (2004). Photochemical modification of cross-linked poly(dimethylsiloxane) by irradiation at 172 nm. *Macromolecules*, 37(16), 5936–5943. <https://doi.org/10.1021/ma049747q>
- Gregoire, F. M., Smas, C. M., & Sul, H. S. (1998). Understanding adipocyte differentiation. *Physiological Reviews*, 78(3), 783–809. <https://doi.org/10.1152/physrev.1998.78.3.783>
- Guneta, V., Loh, Q. L., & Choong, C. (2016). Cell-secreted extracellular matrix formation and differentiation of adipose-derived stem cells in 3D alginate scaffolds with tunable properties. *Journal of Biomedical Materials Research. Part A*, 104(5), 1090–1101. <https://doi.org/10.1002/jbm.a.35644>
- Guneta, V., Zhou, Z., Tan, N. S., Sugii, S., Wong, M. T. C., & Choong, C. (2018). Recellularization of decellularized adipose tissue-derived stem cells: Role of the cell-secreted extracellular matrix in cellular differentiation. *Biomaterials Science*, 6(1), 168–178. <https://doi.org/10.1039/c7bm00695k>
- Gutmann, M., Braun, A., Seibel, J., & Lühmann, T. (2018). Bioorthogonal modification of cell derived matrices by metabolic glycoengineering. *ACS Biomaterials Science and Engineering*, 4(4), 1300–1306. <https://doi.org/10.1021/acsbomaterials.8b00264>
- Hesse, R., Chassé, T., Streubel, P., & Szargan, R. (2004). Error estimation in peak-shape analysis of XPS core-level spectra using UNIFIT 2003: How significant are the results of peak fits? *Surface and Interface Analysis*, 36(10), 1373–1383. <https://doi.org/10.1002/sia.1925>
- Hinderer, S., Shen, N., Ringuette, L. J., Hansmann, J., Reinhardt, D. P., Brucker, S. Y., Davis, E. C., & Schenke-Layland, K. (2015). In vitro elastogenesis: Instructing human vascular smooth muscle cells to generate an elastic fiber-containing extracellular matrix scaffold. *Biomedical Materials*, 10(3), 034102. <https://doi.org/10.1088/1748-6041/10/3/034102>
- Hussey, G. S., Dziki, J. L., & Badylak, S. F. (2018). Extracellular matrix-based materials for regenerative medicine. *Nature Reviews Materials*, 3(7), 159–173. <https://doi.org/10.1038/s41578-018-0023-x>
- Johnson, T. D., Dequach, J. A., Gaetani, R., Ungerleider, J., Elhag, D., Nigam, V., Behfar, A., & Christman, K. L. (2014). Human versus porcine tissue sourcing for an injectable myocardial matrix hydrogel. *Biomaterials Science*, 2(5), 735–744. <https://doi.org/10.1039/c3bm60283d>
- Johnson, T. D., Hill, R. C., Dzieciatkowska, M., Nigam, V., Behfar, A., Christman, K. L., & Hansen, K. C. (2016). Quantification of decellularized human myocardial matrix: A Comparison of six patients. *Proteomics: Clinical Applications*, 10(1), 75–83. <https://doi.org/10.1002/PRCA.201500048>
- Junka, R., Quevada, K., & Yu, X. (2020). Acellular polycaprolactone scaffolds laden with fibroblast/endothelial cell-derived extracellular matrix for bone regeneration. *Journal of Biomedical Materials Research—Part A*, 108(2), 351–364. <https://doi.org/10.1002/JBM.A.36821/FORMAT/PDF>
- Kalluri, R. (2003). Basement membranes: Structure, assembly and role in tumour angiogenesis. *Nature Reviews Cancer*, 3(6), 422–433. <https://doi.org/10.1038/nrc1094>
- Keller, S., Liedek, A., Shendi, D., Bach, M., Tovar, G. E. M., Kluger, P. J., & Southan, A. (2020). Eclectic characterisation of chemically modified cell-derived matrices obtained by metabolic glycoengineering and re-assessment of commonly used methods. *RSC Advances*, 10(58), 35273–35286. <https://doi.org/10.1039/d0ra06819e>
- Keller, S., Wörgötter, K., Liedek, A., Kluger, P. J., Bach, M., Tovar, G. E. M., Tovar, G. E. M., & Southan, A. (2020). Azide-functional extracellular matrix coatings as a bioactive platform for bioconjugation. *ACS Applied Materials and Interfaces*, 12(24), 26868–26879. <https://doi.org/10.1021/acsaami.0c04579>
- Kim, B. S., Kwon, Y. W., Kong, J. S., Park, G. T., Gao, G., Han, W., Kim, M. B., Lee, H., Kim, J. H., & Cho, D. W. (2018). 3D cell printing of in vitro stabilized skin model and in vivo pre-vascularized skin patch using tissue-specific extracellular matrix bioink: A step towards advanced skin tissue engineering. *Biomaterials*, 168, 38–53. <https://doi.org/10.1016/j.biomaterials.2018.03.040>
- Ko, E., Alberti, K., Lee, J. S., Yang, K., Jin, Y., Shin, J., Yang, H. S., Xu, Q., & Cho, S. W. (2016). Nanostructured tendon-derived scaffolds for enhanced bone regeneration by human adipose-derived stem cells. *ACS Applied Materials and Interfaces*, 8(35), 22819–22829. <https://doi.org/10.1021/acsaami.6b05358>
- Köwitsch, A., Zhou, G., & Groth, T. (2018). Medical application of glycosaminoglycans: A review. *Journal of Tissue Engineering and*

- Regenerative Medicine*, 12(1), e23–e41. <https://doi.org/10.1002/term.2398>
- Kshitiz, P. J., Kim, P., Helen, W., Engler, A. J., Levchenko, A., & Kim, D.-H. (2012). Control of stem cell fate and function by engineering physical microenvironments. *Integrative Biology*, 4(9), 1008–1018. <https://doi.org/10.1039/c2ib20080e>
- Leclech, C., Natale, C. F., & Barakat, A. I. (2021). The basement membrane as a structured surface—Role in vascular health and disease. *Journal of Cell Science*, 133(18);jcs239889. <https://doi.org/10.1242/jcs.239889>
- Lu, H., Hoshiba, T., Kawazoe, N., Koda, I., Song, M., & Chen, G. (2011). Cultured cell-derived extracellular matrix scaffolds for tissue engineering. *Biomaterials*, 32(36), 9658–9666. <https://doi.org/10.1016/j.biomaterials.2011.08.091>
- Lu, P., Takai, K., Weaver, V. M., & Werb, Z. (2011). Extracellular matrix degradation and remodeling in development and disease. *Cold Spring Harbor Perspectives in Biology*, 3, a005058. <https://doi.org/10.1101/cshperspect.a005058>
- Magnan, L., Kawecki, F., Labrunie, G., Gluais, M., Izotte, J., Marais, S., Foulc, M.-P., Lafourcade, M., & L'Heureux, N. (2021). In vivo remodeling of human cell-assembled extracellular matrix yarns. *Biomaterials*, 273, 120815. <https://doi.org/10.1016/j.biomaterials.2021.120815>
- Magnan, L., Labrunie, G., Marais, S., Rey, S., Dusserre, N., Bonneau, M., Lacomme, S., Gontier, E., & L'Heureux, N. (2018). Characterization of a cell-assembled extracellular matrix and the effect of the devitalization process. *Acta Biomaterialia*, 82, 56–67. <https://doi.org/10.1016/j.actbio.2018.10.006>
- Malinda, K. M., Nomizu, M., Chung, M., Delgado, M., Kuratomi, Y., Yamada, Y., Kleinman, H. K., & Ponce, M. L. (1999). Identification of laminin α 1 and β 1 chain peptides active for endothelial cell adhesion, tube formation, and aortic sprouting. *The FASEB Journal*, 13(1), 53–62. <https://doi.org/10.1096/fasebj.13.1.53>
- Mecham, R. P. (2012). Overview of extracellular matrix. *Current Protocols in Cell Biology*, 57(Suppl.), 1–16. <https://doi.org/10.1002/0471143030.cb1001s57>
- Miller, A. E., Hu, P., & Barker, T. H. (2020). Feeling things out: Bidirectional signaling of the cell–ECM interface, implications in the mechanobiology of cell spreading, migration, proliferation, and differentiation. *Advanced Healthcare Materials*, 9(8), 1–24. <https://doi.org/10.1002/adhm.201901445>
- Mrsic, I., Bäuerle, T., Ullitsch, S., Lorenz, G., Rebner, K., Kandelbauer, A., & Chassé, T. (2021). Oxygen plasma surface treatment of polymer films—Pellethane 55DE and EPR-g-VTMS. *Applied Surface Science*, 536, 147782. <https://doi.org/10.1016/j.apsusc.2020.147782>
- Myllyharju, J., & Kivirikko, K. I. (2004). Collagens, modifying enzymes and their mutations in humans, flies and worms. *Trends in Genetics*, 20(1), 33–43. <https://doi.org/10.1016/j.tig.2003.11.004>
- Nellinger, S., Schmidt, I., Heine, S., Volz, A. C., & Kluger, P. J. (2020). Adipose stem cell-derived extracellular matrix represents a promising biomaterial by inducing spontaneous formation of prevascular-like structures by mvECs. *Biotechnology and Bioengineering*, 117(10), 3160–3172. <https://doi.org/10.1002/bit.27481>
- Novosevskaya, E. S., Grigorieva, O. A., Efimenko, A. Y., & Kalinina, N. I. (2019). Extracellular matrix in the regulation of stem cell differentiation. *Biochemistry*, 84(3), 232–240. <https://doi.org/10.1134/S0006297919030052>
- Pati, F., Ha, D. H., Jang, J., Han, H. H., Rhie, J. W., & Cho, D. W. (2015). Biomimetic 3D tissue printing for soft tissue regeneration. *Biomaterials*, 62, 164–175. <https://doi.org/10.1016/j.biomaterials.2015.05.043>
- Pati, F., Jang, J., Ha, D. H., Won Kim, S., Rhie, J. W., Shim, J. H., Kim, D. H., & Cho, D. W. (2014). Printing three-dimensional tissue analogues with decellularized extracellular matrix bioink. *Nature Communications*, 5(1), 1–11. <https://doi.org/10.1038/ncomms4935>
- Pierleoni, C., Verdenelli, F., Castellucci, M., & Cinti, S. (1998). Fibronectins and basal lamina molecules expression in human subcutaneous white adipose tissue. *European Journal of Histochemistry*, 42(3), 183–188. <https://europemc.org/article/med/9857243>
- Ponce, M. L., Nomizu, M., Delgado, M. C., Kuratomi, Y., Hoffman, M. P., Powell, S., Yamada, Y., Kleinman, H. K., & Malinda, K. M. (1999). Identification of endothelial cell binding sites on the laminin γ 1 chain. *Circulation Research*, 84(6), 688–694. <https://doi.org/10.1161/01.RES.84.6.688>
- Randles, M. J., Humphries, M. J., & Lennon, R. (2017). Proteomic definitions of basement membrane composition in health and disease. *Matrix Biology*, 57–58, 12–28. <https://doi.org/10.1016/j.matbio.2016.08.006>
- Rossi, E., Guerrero, J., Aprile, P., Tocchio, A., Kappos, E. A., Gerges, I., Lenardi, C., Martin, I., & Scherberich, A. (2018). Decoration of RGD-mimetic porous scaffolds with engineered and devitalized extracellular matrix for adipose tissue regeneration. *Acta Biomaterialia*, 73, 154–166. <https://doi.org/10.1016/j.actbio.2018.04.039>
- Rousselle, P., Montmasson, M., & Garnier, C. (2019). Extracellular matrix contribution to skin wound re-epithelialization. *Matrix Biology*, 75–76, 12–26.
- Ruff, S. M., Keller, S., Wieland, D. E., Wittmann, V., Tovar, G. E. M., Bach, M., & Kluger, P. J. (2017). clickECM: Development of a cell-derived extracellular matrix with azide functionalities. *Acta Biomaterialia*, 52, 159–170. <https://doi.org/10.1016/j.actbio.2016.12.022>
- Salbach, J., Rachner, T. D., Rauner, M., Hempel, U., Anderegg, U., Franz, S., Simon, J.-C., Lorenz, & Hofbauer, C. (2012). Regenerative potential of glycosaminoglycans for skin and bone. *Journal of Molecular Medicine*, 90, 625–635. <https://doi.org/10.1007/s00109-011-0843-2>
- Schenke-Layland, K., Rofail, F., Heydarkhan, S., Gluck, J. M., Ingle, N. P., Angelis, E., Choi, C. H., MacLellan, W. R., Beygui, R. E., Shemin, R. J., & Heydarkhan-Hagvall, S. (2009). The use of three-dimensional nanostructures to instruct cells to produce extracellular matrix for regenerative medicine strategies. *Biomaterials*, 30(27), 4665–4675. <https://doi.org/10.1016/j.biomaterials.2009.05.033>
- Shendi, D., Marzi, J., Linthicum, W., Rickards, A. J., Dolivo, D. M., Keller, S., Kaus, M. A., Wen, Q., McDevitt, T. C., Dominko, T., Schenke-Layland, K., & Rolle, M. W. (2019). Hyaluronic acid as a macromolecular crowding agent for production of cell-derived matrices. *Acta Biomaterialia*, 100, 292–305. <https://doi.org/10.1016/j.actbio.2019.09.042>
- Shi, Z., Neoh, K. G., Kang, E. T., Poh, C. K., & Wang, W. (2014). Enhanced endothelial differentiation of adipose-derived stem cells by substrate nanotopography. *Journal of Tissue Engineering and Regenerative Medicine*, 8(1), 50–58. <https://doi.org/10.1002/term.1496>
- Si, Z., Wang, X., Sun, C., Kang, Y., Xu, J., Wang, X., & Hui, Y. (2019). Adipose-derived stem cells: Sources, potency, and implications for regenerative therapies. *Biomedicine and Pharmacotherapy*, 114, 108765. <https://doi.org/10.1016/j.biopha.2019.108765>
- Song, M., Liu, Y., & Hui, L. (2018). Preparation and characterization of acellular adipose tissue matrix using a combination of physical and chemical treatments. *Molecular Medicine Reports*, 17(1), 138–146. <https://doi.org/10.3892/mmr.2017.7857>
- Subbiah, R., Hwang, M. P., Du, P., Suhaeri, M., Hwang, J.-H., Hong, J.-H., & Park, K. (2016). Tunable crosslinked cell-derived extracellular matrix guides cell fate. *Macromolecular Bioscience*, 16(11), 1723–1734. <https://doi.org/10.1002/mabi.201600280>
- Sun, Y., Yan, L., Chen, S., & Pei, M. (2018). Functionality of decellularized matrix in cartilage regeneration: A comparison of tissue versus cell sources. *Acta Biomaterialia*, 74, 56–73. <https://doi.org/10.1016/j.actbio.2018.04.048>

- Sutherland, A. J., Converse, G. L., Hopkins, R. A., & Detamore, M. S. (2015). The bioactivity of cartilage extracellular matrix in articular cartilage regeneration. *Advanced Healthcare Materials*, 4(1), 29–39. <https://doi.org/10.1002/ADHM.201400165>
- Tan, Q. W., Zhang, Y., Luo, J. C., Zhang, D., Xiong, B. J., Yang, J. Q., Xie, H. Q., & Lv, Q. (2017). Hydrogel derived from decellularized porcine adipose tissue as a promising biomaterial for soft tissue augmentation. *Journal of Biomedical Materials Research—Part A*, 105(6), 1756–1764. <https://doi.org/10.1002/jbm.a.36025>
- Theocharis, A. D., Skandalis, S. S., Gialeli, C., & Karamanos, N. K. (2016). Extracellular matrix structure. *Advanced Drug Delivery Reviews*, 97, 4–27. <https://doi.org/10.1016/j.addr.2015.11.001>
- Thomas-Porch, C., Li, J., Zanata, F., Martin, E. C., Pashos, N., Genemaras, K., Poche, J. N., Totaro, N. P., Bratton, M. R., Gaupp, D., Frazier, T., Wu, X., Ferreira, L. M., Tian, W., Wang, G., Bunnell, B. A., Flynn, L., Hayes, D., & Gimble, J. M. (2018). Comparative proteomic analyses of human adipose extracellular matrices decellularized using alternative procedures. *Journal of Biomedical Materials Research—Part A*, 106(9), 2481–2493. <https://doi.org/10.1002/jbm.a.36444>
- Turner, A. E. B., Yu, C., Bianco, J., Watkins, J. F., & Flynn, L. E. (2012). The performance of decellularized adipose tissue microcarriers as an inductive substrate for human adipose-derived stem cells. *Biomaterials*, 33(18), 4490–4499. <https://doi.org/10.1016/j.biomaterials.2012.03.026>
- Volz, A. C., Huber, B., Schwandt, A. M., & Kluger, P. J. (2017). EGF and hydrocortisone as critical factors for the co-culture of adipogenic differentiated ASCs and endothelial cells. *Differentiation*, 95, 21–30. <https://doi.org/10.1016/j.diff.2017.01.002>
- Wagner, C. D. (1983). Sensitivity factors for XPS analysis of surface atoms. *Journal of Electron Spectroscopy and Related Phenomena*, 32(2), 99–102. [https://doi.org/10.1016/0368-2048\(83\)85087-7](https://doi.org/10.1016/0368-2048(83)85087-7)
- Wang, L., Johnson, J. A., Zhang, Q., & Beahm, E. K. (2013). Combining decellularized human adipose tissue extracellular matrix and adipose-derived stem cells for adipose tissue engineering. *Acta Biomaterialia*, 9(11), 8921–8931. <https://doi.org/10.1016/j.actbio.2013.06.035>
- Wang, Z., Lin, M., Xie, Q., Sun, H., Huang, Y., Zhang, D. D., Yu, Z., Bi, X., Chen, J., Wang, J., Shi, W., Gu, P., & Fan, X. (2016). Electrospun silk fibroin/poly(lactide-co-ε-caprolactone) nanofibrous scaffolds for bone regeneration. *International Journal of Nanomedicine*, 11, 1483–1500. <https://doi.org/10.2147/IJN.S97445>
- Wei, H. J., Liang, H. C., Lee, M. H., Huang, Y. C., Chang, Y., & Sung, H. W. (2005). Construction of varying porous structures in acellular bovine pericardium as a tissue-engineering extracellular matrix. *Biomaterials*, 26(14), 1905–1913. <https://doi.org/10.1016/j.biomaterials.2004.06.014>
- Wolf, M. T., Daly, K. A., Brennan-Pierce, E. P., Johnson, S. A., Carruthers, C. A., D'Amore, A., Nagarkar, S. P., Velankar, S. S., & Badylak, S. F. (2012). A hydrogel derived from decellularized dermal extracellular matrix. *Biomaterials*, 33(29), 7028–7038. <https://doi.org/10.1016/j.biomaterials.2012.06.051>
- Xing, H., Lee, H., Luo, L., & Kyriakides, T. R. (2020). Extracellular matrix-derived biomaterials in engineering cell function. *Biotechnology Advances*, 42, 107421. <https://doi.org/10.1016/j.biotechadv.2019.107421>
- Young, D. A., Ibrahim, D. O., Hu, D., & Christman, K. L. (2011). Injectable hydrogel scaffold from decellularized human lipoaspirate. *Acta Biomaterialia*, 7(3), 1040–1049. <https://doi.org/10.1016/j.actbio.2010.09.035>
- Yurchenco, P. D., & Schittny, J. C. (1990). Molecular architecture of basement membranes. *The FASEB Journal*, 4(6), 1577–1590. <https://doi.org/10.1096/fasebj.4.6.2180767>

SUPPORTING INFORMATION

Additional supporting information may be found in the online version of the article at the publisher's website.

How to cite this article: Nellinger, S., Mrcic, I., Keller, S., Heine, S., Southan, A., Bach, M., Volz, A.-C., Chassé, T., & Kluger, P. J. (2022). Cell-derived and enzyme-based decellularized extracellular matrix exhibit compositional and structural differences that are relevant for its use as a biomaterial. *Biotechnology and Bioengineering*, 119, 1142–1156. <https://doi.org/10.1002/bit.28047>